Letter

Vol. 43, No. 21 / 1 November 2018 / *Optics Letters* 5439

Optics Letters

Performance enhancement of an optically-injected-semiconductor-laser-based optoelectronic oscillator by subharmonic microwave modulation

PEI ZHOU,[1] FANGZHENG ZHANG,* DAOCHENG ZHANG,[1] AND SHILONG PAN[1,2]

[1]Key Laboratory of Radar Imaging and Microwave Photonics, Ministry of Education, Nanjing University of Aeronautics and Astronautics, Nanjing 210016, China
[2]e-mail: pans@nuaa.edu.cn
*Corresponding author: zhangfangzheng@nuaa.edu.cn

Received 14 August 2018; revised 29 September 2018; accepted 9 October 2018; posted 9 October 2018 (Doc. ID 342313); published 30 October 2018

An approach to enhancing the performance of an optically-injected-semiconductor-laser-based optoelectronic oscillator (OEO) is proposed by subharmonic microwave modulation. A free-running OEO is first established based on period-one dynamics of an optically injected semiconductor laser. The oscillation frequency can be tuned in the range of 8.87 to 18.41 GHz by controlling the injection strength, but the output signal suffers from strong side modes and poor frequency stability. To address these problems, subharmonic microwave modulation is applied to the injected semiconductor laser. In the experiment, microwave modulation with 1/2, 1/4, and 1/6 subharmonics is demonstrated. The side-mode suppression ratio is improved by over 40 dB, while the phase noise at a 1 kHz offset is reduced by about 18 dB. Furthermore, the frequency drift over a period of 20 min, which characterizes the long-term stability, is reduced from 8.7 kHz to less than 1 Hz, indicating a significant reduction of over three orders.

https://doi.org/10.1364/OL.43.005439

Microwave signal generators have wide applications in radar, satellite communication, and many other emerging areas [1–3]. The microwave signal generated by electronic resonators suffers from poor phase noise, especially in the high frequency range. Fortunately, the optoelectronic oscillator (OEO) provides a promising solution to produce microwave signals with a high frequency and very low phase noise by constructing an ultra-high Q-factor cavity realized by a low-loss fiber [4]. Typically, the frequency of an OEO is determined by an electrical bandpass filter (EBPF) within its cavity. Although a long cavity can help to achieve a low phase noise, it would result in the generation of many densely spaced side modes, making it difficult for a commercial EBPF to suppress all the undesired side modes. As for frequency tunability of an OEO, it can be realized by replacing the EBPF with a single-passband microwave photonic filter (MPF), which usually has a relatively large frequency tuning range [5]. While broadly tunable, a single-passband MPF usually has a much larger bandwidth than that of an EBPF and, therefore, is unable to largely suppress the side modes in a long-cavity OEO. In order to improve the side-mode suppression ratio (SMSR), OEOs with multiple loops have been proposed [6]. In this configuration, two or more optoelectronic feedback loops with different lengths are incorporated to suppress the side modes by using the associated Vernier filtering which arises from this configuration. Based on a similar principle, several multi-loop OEOs have been demonstrated by adding an additional electrical loop, optical loop, or fiber laser loop (i.e., coupled OEO). However, the side modes supported by both the long and short loops still exist, making it hard to further enhance the SMSR.

In a typical OEO, the fiber and other devices in its cavity are sensitive to environments, e.g., the temperature-change-induced index variation of a standard single-mode fiber (SMF) is on the order of 10 ppm/K. Therefore, the frequency accuracy and stability of a free-running OEO are limited. In particular, the phase noise performance at low offset frequencies of a free-running OEO is inferior due to its sensitivity to the environment. To deal with this problem, several passive stabilization methods have been reported, such as thermal stabilization, vibration isolation, and the use of temperature-insensitive photonic bandgap fiber [7]. Stabilization of an OEO with injection-locking [8] or phase-locked loop (PLL) [9] techniques has also been investigated. For schemes using injection locking, a stable microwave oscillator with the same frequency as the OEO is required, which dramatically increases the cost of the system when a high-frequency output is required. For schemes using the PLL's, complicated electrical circuits and frequency dividers with a high division factor are required, making the system complex and expensive.

In this Letter, we demonstrate an approach to enhance the performance of a tunable OEO by subharmonic microwave modulation. The OEO is established based on the period-one (P1) dynamics of an optically injected semiconductor laser [10–15]. By changing the optical injection strength, its oscillation frequency can be tuned in the range of 8.87 to 18.41 GHz. However, the output signal suffers from large side modes and poor frequency stability. To address this problem, external subharmonic modulation is introduced to stabilize the generated microwave signal. In the experimental demonstration, stabilization of the tunable OEO by applying 1/2, 1/4, or 1/6 subharmonic microwave modulation to the semiconductor laser is verified. Compared with the free-running OEO without stabilization, the SMSR is improved by over 40 dB. The phase noise at a 1 kHz offset is reduced by about 18 dB. Furthermore, the frequency drift over a period of 20 min, which characterizes the long-term stability, is reduced from 8.7 kHz to less than 1 Hz, indicating a significant reduction of over three orders. These results show that the proposed approach is effective for side-mode suppression and frequency stabilization of the tunable OEO.

The schematic diagram of the proposed OEO is shown in Fig. 1. It consists of a master laser (ML), a polarization controller (PC), an optical circulator (CIR), a slave laser (SL), a 90:10 optical coupler (OC), a section of SMF, a photodetector (PD), an electrical amplifier (EA), a 10 dB directional coupler (EC1), a 1:1 electrical coupler (EC2), and a microwave synthesizer (MS). In this system, a single-mode semiconductor laser is used as the SL. The continuous wave (CW) light from the ML is injected into the slave laser. To maximize the injection efficiency, the polarization of the injection light and the SL are matched through a PC before the CIR. After proper optical injection, the P1 oscillation state can be excited through undamping the relaxation resonance [10]. The output intensity of the injected SL shows self-sustained intensity oscillation. Its optical spectrum exhibits highly asymmetric double-sideband modulation, and the modulation frequency equals the P1 frequency f_o. A microwave signal can be obtained with a frequency of f_o after photodetection. By varying the injection strength ξ and/or the detuning frequency f_i, the P1 frequency f_o can be tuned by as much as 100 GHz [11]. Here f_i equals the frequency difference between the master and free-running SL, and the injection strength ξ is defined as the square root of the power ratio between the injection light and the free-running SL. The injection power is measured at the output port of the circulator connected to the SL (port 2). Although broadly

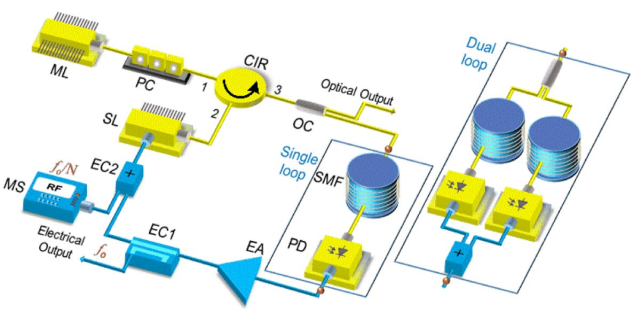

Fig. 1. Schematic diagram of the tunable OEO with subharmonic microwave modulation stabilization. ML, master laser; PC, polarization controller; CIR, optical circulator; SL, slave laser; OC, optical coupler; PD, photodetector; EA, electrical amplifier; EC, electrical coupler; MS, microwave synthesizer.

tunable, the generated signal has a large linewidth of 10–100 MHz, which mainly arises from the spontaneous emission noise of the injected laser [12]. To narrow the linewidth, a method of optical feedback has been demonstrated, which generated microwave signals up to 45.4 GHz with a linewidth around 10 kHz [13,14]. In order to further reduce the linewidth and phase noise, an optoelectronic feedback loop is applied to construct an OEO [15]. In this system, a portion of the optical output after the CIR is delayed by a span of fiber and then sent to a PD. Afterwards, the obtained microwave signal is amplified by an EA. Before being fed back to modulate the SL, a 10 dB directional coupler is inserted to tap 10% of the signal power for measurement. Thus, a tunable OEO is established, and frequency tuning is achieved through controlling f_i and/or ξ.

The output signal from this OEO would suffer from large side modes and poor frequency stability [15]. To enhance the performance, a MS with a frequency of f_o/N (N is an integer) is employed to implement subharmonic microwave modulation. The subharmonic microwave modulation signal is fed into the OEO loop and applied to the SL via the 1:1 electrical coupler (EC2). One of the Nth-order modulation sidebands of the cavity resonance wavelength is located near the injection light and locks it, and vice versa. Therefore, the P1 oscillation frequency (i.e., OEO oscillation frequency f_o) is locked. In the OEO cavity, only the OEO mode closest to the Nth-order modulation sideband will be locked. As a result, the OEO oscillation will be stabilized and a stable single-mode signal can be generated.

An experiment based on the setup depicted in Fig. 1 was performed. A laser source (TeraXion PS-TNL) with a wavelength of 1543.644 nm is applied as the ML. The SL (Actech LD15DM) is a distributed feedback (DFB) laser biased at 31.9 mA, about five times that of its threshold. Its free-running wavelength and power are 1543.666 nm and 3.19 dBm, respectively. The modulation bandwidth of SL was measured to be ∼12.3 GHz. In the experiment, the master-slave detuning frequency was fixed at 2.8 GHz. In the OEO cavity, the SMF is 1 km long. The PD has a bandwidth of 18 GHz and a responsivity of 0.85 A/W. Two cascaded EAs with a total RF gain of ∼40 dB and an operation bandwidth of 8–18 GHz were used for signal amplification. The microwave modulation signal was generated by an MS (Agilent N5183B). At the optical output, the optical spectrum was monitored by an optical spectrum analyzer (OSA, Yokogawa AQ6370C). The electrical spectral properties were measured by a 50 GHz electrical spectrum analyzer (ESA, R&S RSWP-50).

Initially, microwave modulation was not applied, as captured in Fig. 2(a), where the measured output frequency as a function of injection strength is shown. In obtaining the result in Fig. 2(a), the injection strength is tuned by adjusting the optical power of the ML. It is observed that when the injection strength ξ increases from 0.22 to 1.04, the oscillation frequency f_o of the OEO can be tuned from 8.87 to 18.41 GHz. The corresponding electrical spectra of the output signals at different frequencies are given in Fig. 2(b). It should be noted that the frequency tuning range is mainly limited by the bandwidth of the EA and PD. By using devices with larger bandwidths, the tuning range of our approach could be further extended.

A 17.45 GHz microwave signal can be generated by the OEO when ξ equals 0.95. Its electrical spectrum was measured

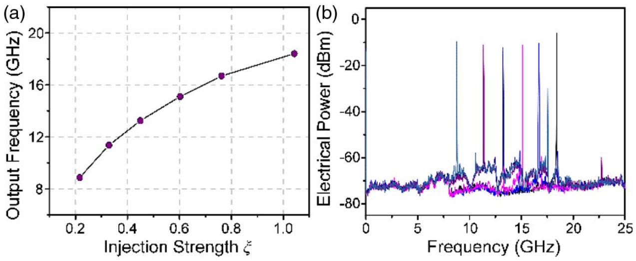

Fig. 2. (a) Measured output frequency as a function of the injection strength and (b) electrical spectra of the generated microwave signal at different frequencies.

and shown in Fig. 3(a), where many side modes separated by ∼200 kHz are observed. As can be seen, the SMSR is only 22.5 dB. After adopting a 1/2 subharmonic microwave modulation, i.e., the modulation frequency equals $f_o/2 = 8.725$ GHz, the output signal of the OEO becomes stably locked. The locking threshold of the input power of the $f_o/2$ signal is ∼13.5 dBm. Here the input power was set to be 15 dBm. As shown in Fig. 3(b), the undesired side modes are effectively suppressed and the SMSR reaches 65.4 dB. Compared with the free-running OEO, the OEO with $f_o/2$ modulation achieves a 42.9 dB improvement of the SMSR. It should be noted that when the input power was fixed at 15 dBm, the locking range of the input modulation frequency was about 0.14 MHz around $f_o/2$ in the experiment. The largest SMSR is achieved when the modulation frequency equals $f_o/2$. As shown in Fig. 1, to further suppress the undesired side modes, a dual-loop structure was adopted, where a span of SMF and a PD were used in each loop [6]. After the PDs, the obtained signals were electrically combined in an EC. In the experiment, the two SMFs in the dual-loop structure are 1 and 1.5 km long. Figure 3(c) shows the electrical spectrum of the 17.45 GHz microwave signal generated by the free-running dual-loop OEO. Thanks to the Vernier effect, the SMSR is increased to 66.5 dB when both loops are enabled.

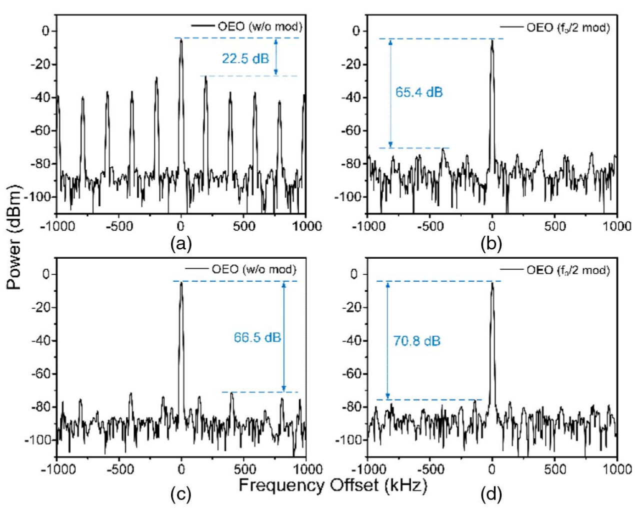

Fig. 3. Measured electrical spectra of the generated 17.45 GHz signal. (a) Free-running single-loop OEO, (b) single-loop OEO with $f_o/2$ modulation, (c) free-running dual-loop OEO, and (d) dual-loop OEO with $f_o/2$ modulation. (Span, 2 MHz; RBW, 10 kHz).

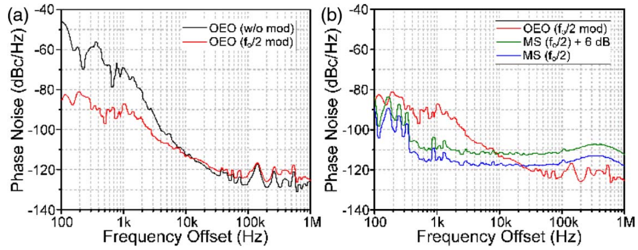

Fig. 4. Comparison of the SSB phase noise spectra. (a) Free-running OEO (black) and OEO with $f_o/2$ modulation (red); (b) OEO with $f_o/2$ modulation (red), ideally frequency-doubled signal (green), and $f_o/2$ signal from the MS (blue).

Figure 3(d) shows the result when $f_o/2$ modulation is enabled. The measured SMSR of the OEO is further improved to 70.8 dB, and all the side modes are well suppressed.

The single-sideband (SSB) phase noise performance of the generated signal was also investigated. Figure 4(a) shows the phase noise measurement results of the generated 17.45 GHz signal by the dual-loop OEO without external modulation (black) and the OEO with $f_o/2$ modulation (red). As can be seen, the phase noise of the free-running dual-loop OEO is poor at offset frequencies lower than 10 kHz. Specifically, the free-running OEO has a phase noise of −69.15 dBc/Hz at 1 kHz offset. This relatively high phase noise at low offset frequencies of OEO is caused by its sensitivity to the environmental perturbations. After adopting the $f_o/2$ subharmonic modulation, the SSB phase noise of the stabilized OEO has been greatly improved at low offset frequencies, while the phase noise at high offset frequencies remains almost unchanged. As can be seen, the phase noise of the stabilized dual-loop OEO with $f_o/2$ modulation reaches −87.13 dBc/Hz at 1 kHz offset, which is ∼18 dB lower than that of the free-running dual-loop OEO. Figure 4(b) shows the SSB phase noise spectra of the OEO with $f_o/2$ modulation (red), the ideally frequency-doubled signal (from $f_o/2$ to f_o, green) and the $f_o/2$ signal from the MS (blue). The phase noise of the ideally frequency-doubled signal is obtained by adding 6 dB to the phase noise of the $f_o/2$ modulation signal [3]. It can be seen that the stabilized OEO has the best performance at offset frequencies above 10 kHz, while the phase noise at low offset frequencies is higher than that of the ideally frequency-doubled signal, which is due to the flicker noise of the system [16]. By reducing the flicker noise, e.g., using a low-phase-noise amplifier and other low-noise devices, the phase noise of the stabilized OEO at offset frequencies below 10 kHz can be further suppressed.

The SSB phase noises of the stabilized OEO with $f_o/2$ modulation were also measured under different frequencies. Figure 5 shows the measured phase noises at 1, 10, and 100 kHz as a function of the OEO frequency. As can be seen, the phase noise is between −80.20 and −87.25 dBc/Hz at 1 kHz, between −108.16 and −114.04 dBc/Hz at 10 kHz, and between −118.64 and −127.35 at 100 kHz, respectively. Therefore, the phase noise of the stabilized OEO shows limited fluctuations, as the output frequency is tuned.

Long-term frequency stability was investigated by measuring frequency drifts over a period of 20 min, which was performed using the "max hold" function on the ESA. As shown in Fig. 6(a), the peak frequency of the 12.45 GHz free-running

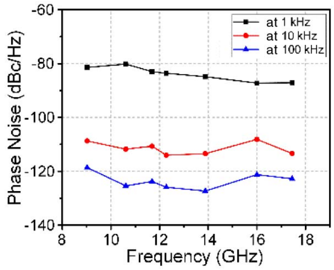

Fig. 5. Phase noises at 1 (black), 10 (red), and 100 kHz (blue) of the stabilized OEO for different frequencies.

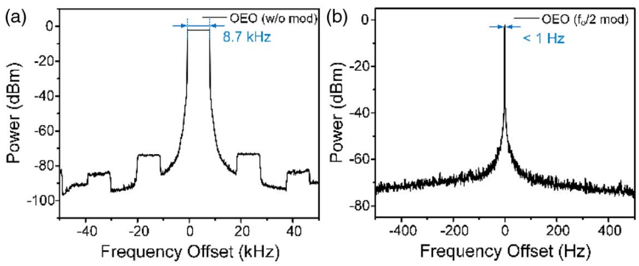

Fig. 6. Traces of microwave frequency drifts for an observation period of 20 min. (a) Free-running dual-loop OEO (span, 100 kHz; RBW, 100 Hz). (b) Dual-loop OEO with $f_o/2$ modulation (span, 1 kHz; RBW, 1 Hz).

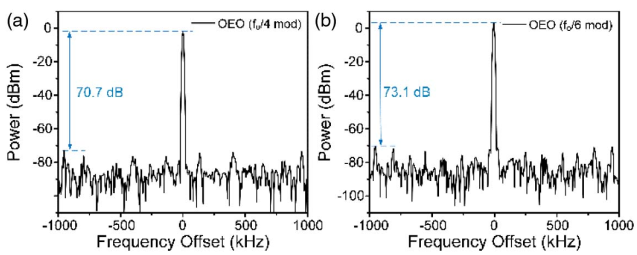

Fig. 7. Measured electrical spectra. (a) 12.45 GHz OEO with $f_o/4$ modulation and (b) 11.37 GHz OEO with $f_o/6$ modulation. (Span, 2 MHz; RBW, 10 kHz).

dual-loop OEO drifts by about 8.7 kHz for an observation period of 20 min. In contrast, with the aid of $f_o/2$ modulation, no obvious frequency drifts are observed over a time period of 20 min. As shown in Fig. 6(b), the frequency drift of the peak frequency is less than 1 Hz for the stabilized OEO. The frequency drifts of the $f_o/2$ signal and the f_o signal from the MS were also measured, and both were found to be less than 1 Hz. These results indicate that the frequency drift of the stabilized OEO over a period of 20 min is significantly reduced by over three orders, compared with the free-running OEO.

The electrical spectra of the generated microwave signals at different frequencies which are modulated by different subharmonics, i.e., 1/4 and 1/6 subharmonics, were also evaluated. Without loss of generality, Fig. 7 shows the measured electrical spectra of (a) a 12.45 GHz dual-loop OEO with $f_o/4$ modulation and (b) a 11.37 GHz dual-loop OEO with $f_o/6$ modulation. The measured SMSR is 70.71 dB and 73.1 dB, respectively. These results show that the proposed stabilization approach is effective for the tunable OEO through modulation of different subharmonics.

In conclusion, we have demonstrated an approach to enhance the performance of an optically-injected-semiconductor-laser-based OEO by subharmonic microwave modulation. Compared to a free-running single-loop OEO, the SMSR is improved by over 40 dB by applying subharmonic microwave modulation. The phase noise at a 1 kHz offset was reduced by about 18 dB, and the frequency drift over a period of 20 min was reduced from 8.7 kHz to less than 1 Hz. The phase noise of the stabilized OEO can be maintained, as the frequency is continuously tuned. The stabilization of the tunable OEO at different frequencies by modulation with different subharmonics was also verified. The results show that the proposed approach is effective for side-mode suppression and frequency stabilization of the tunable OEO. Compared with previous schemes, our method does not require a high-frequency frequency divider, microwave oscillator, or modulator, leading to a significant reduction in the cost and complexity.

Funding. Natural Science Foundation of Jiangsu Province (SBK2018030017); National Natural Science Foundation of China (NSFC) (61527820, 61871214); Fundamental Research Funds for the Central Universities (NS2018028); Jiangsu Provincial Program for High-level Talents in Six Areas (DZXX-005).

REFERENCES

1. F. Z. Zhang, Q. S. Guo, Z. Q. Wang, P. Zhou, G. Q. Zhang, J. Sun, and S. L. Pan, Opt. Express **25**, 16274 (2017).
2. S. L. Pan, D. Zhu, S. F. Liu, K. Xu, Y. T. Dai, T. L. Wang, J. G. Liu, N. H. Zhu, Y. Xue, and N. J. Liu, IEEE Microw. Mag. **16**(8), 61 (2015).
3. G. J. Schneider, J. A. Murakowski, C. A. Schuetz, S. Shi, and D. W. Prather, Nat. Photonics **7**, 118 (2013).
4. X. S. Yao and L. Maleki, J. Opt. Soc. Am. B **13**, 1725 (1996).
5. W. Li and J. P. Yao, IEEE Trans. Microw. Theory Tech. **60**, 1735 (2012).
6. X. S. Yao and L. Maleki, IEEE J. Quantum Electron. **36**, 79 (2000).
7. M. Kaba, H.-W. Li, A. S. Daryoush, J.-P. Vilcot, D. Decoster, J. Chazelas, G. Bouwmans, Y. Quiquempois, and F. Deborgies, IEEE Microw. Mag. **7**(4), 38 (2006).
8. M. Fleyer, A. Sherman, M. Horowitz, and M. Namer, Opt. Lett. **41**, 1993 (2016).
9. Y. Zhang, D. Hou, and J. Zhao, J. Lightwave Technol. **32**, 2408 (2014).
10. S. K. Hwang, J. M. Liu, and J. K. White, IEEE J. Sel. Top. Quantum Electron. **10**, 974 (2004).
11. P. Zhou, F. Z. Zhang, Q. S. Guo, S. M. Li, and S. L. Pan, IEEE J. Sel. Top. Quantum Electron. **23**, 1801109 (2017).
12. S. C. Chan and J. M. Liu, IEEE J. Sel. Top. Quantum Electron. **10**, 1025 (2004).
13. J. P. Zhuang and S. C. Chan, Opt. Lett. **38**, 344 (2013).
14. J. P. Zhuang and S. C. Chan, Opt. Express **23**, 2777 (2015).
15. J. Suelzer, T. B. Simpson, P. S. Devgan, and N. G. Usechak, Opt. Lett. **42**, 3181 (2017).
16. W. Zhou, O. Okusaga, E. Levy, J. Cahill, A. Docherty, C. Menyuk, G. Cater, and M. Horowitz, Proc. SPIE **8255**, 82551N (2012).